APPENDIX: Genotypic variation in parasite avoidance behavior and other mechanistic, non-linear components of transmission

Alexander T. Strauss[1,2] (straussa@umn.edu), Jessica L. Hite[1,3] (jhite2@unl.edu), David J. Civitello[4] (david.james.civitello@emory.edu), Marta S. Shocket[1,5] (mshocket@standford.edu), Carla E. Cáceres[6] (cecacere@illinois.edu), and Spencer R. Hall[1] (sprhall@indiana.edu)

[1]Department of Biology, Indiana University, Bloomington, IN 47401, USA

[2]Present address: Department of Ecology, Evolution, and Behavior, University of Minnesota, St. Paul, MN 55108, USA

[3]Present address: Department of Biological Sciences, University of Nebraska at Lincoln, Lincoln, NE 68588, USA

[4]Department of Biology, Emory University, Atlanta, GA 30322, USA

[5]Present address: Department of Biology, Stanford University, Stanford, CA 94305

[6]School of Integrative Biology, University of Illinois at Urbana-Champaign, Urbana, IL 61801, USA

APPENDIX

In this appendix, we provide additional methodological details and results. First, we present a traditional statistical analysis that reiterates the most basic results from the main text (Table S1). Next, we show that consumption of algae serves as an accurate proxy for consumption of *M. bicuspidata* parasites by *D. dentifera* hosts (Fig. S1). Then, we explain additional details of the model fitting and display the best transmission model fit to all host genotypes in all rounds of the experiment (Figs. S2-S4; analogous to Fig. 1 in the main text but including all host genotypes). We also list all of the parameter estimates along with their bootstrapped 95% confidence intervals (Tables S2-S4). Then, we display the two remaining correlations among parameters (Fig. S5; complementing the stronger correlations shown in Fig. 3 in the main text), we graphically show the round-to-round variation for genotypes that were

repeated among rounds (Fig. S6), and we report all of the Spearman correlation statistics (Table S4). Finally, we confirm that host mortality prior to diagnosis did not bias our results.

Traditional analysis using generalized linear models

To complement the model fitting in the main text, we also present a more traditional statistical analysis. We fit two separate generalized linear models, one to the size-specific foraging data (assuming normally distributed residuals) and one to the infection data (assuming binomially distributed residuals), using the lme4 package in R (Bates *et al.* 2015; R Core Team 2017). Size specific foraging rate ($\hat{f}$) was calculated as $\hat{f} = \ln\left(\frac{ungrazed\ A}{grazed\ A}\right)\frac{V}{tL^2}$, where *A* is the *in vivo* fluorescence of algae, *V* is the volume of tubes used in the experiment, *t* is the duration of the assay, and *L* is the body size of the host (Sarnelle & Wilson 2008). In both statistical models, we tested for effects of host genotype, the density of parasites, round of the experiment, and two-way interactions between host genotype and both parasite density and round. We summarized results with analysis of deviance tables (Table S1) using type II sums of squares and chi square tests in the statistical package car (Fox & Weisberg 2011). We confirmed that residuals of the foraging model did not deviate from normality with a Shapiro-Wilk test ($p = 0.83$).

All terms and interactions were highly significant for the size-specific foraging rate model (all $p < 0.0001$). Thus, foraging rates differed among genotypes, parasite densities, and rounds of the experiment, and genotypes differed in their foraging rates at different parasite densities and in different rounds. Infections differed significantly among genotypes and parasite densities (both $p < 0.0001$) and marginally among rounds ($p = 0.068$). Interactions between genotype and parasite density ($p = 0.96$) and genotype and round ($p = 0.72$) were relatively unimportant for the infection model. Note that unlike the fitted dynamical models in the main text, these results of the generalized linear infection model cannot account for variation in exposure rates (i.e., genotypes with faster foraging rates encountered more parasite

spores, which all else equal, increased their probability of becoming infected). Broadly however, results of the generalized linear models reiterate the most basic results of the model competition in the main text (Table 2).

Table S1. *Analysis of deviance table for generalized linear models.*

parameter	df	size-specific foraging rate		infection	
		χ^2	*p*	χ^2	*p*
genotype	18	188.4	<0.0001	80.4	<0.0001
parasite density	1	563.1	<0.0001	130.8	<0.0001
round	2	42.5	<0.0001	5.4	0.068
genotype * parasite density	18	94.0	<0.0001	8.9	0.96
genotype * round	2	119.2	<0.0001	3.7	0.72

Consumption of algae as a proxy for consumption of parasites

A previous experiment confirmed that consumption of algae provides an accurate proxy for consumption of *M. bicuspidata* spores. In short, we calculated foraging rates both in terms of the consumption of algal *A* (f_A: as in the main text) and consumption of parasites *Z* (f_Z). We confirmed that foraging rates were very similar when calculated either way ($f_A \approx f_Z$).

First, we calculated foraging rates in terms of algal consumption (f_A). As in the main experiment, we isolated hosts in tubes (12 mL) and allowed them to forage (7 hours). We created a gradient of foraging rates by varying host age (4, 6, 10, 15, or 18 days) and parasite density (75 or 250 spores/mL), using a single host genotype. We replicated each combination of host age and spore density 5-10 times (86 total replicates). Ungrazed control tubes received the same inoculation of algae and spores but did not include a host (replicated 12x at each parasite density). As in the main experiment, we calculated foraging rate in terms of relative algal fluorescence: $f_A = \ln\left(\frac{ungrazed\ A}{grazed\ A}\right)\frac{V}{t}$, where *A* is the *in vivo* fluorescence of algae, *V*

is the volume of tubes used in the experiment, and t is the duration of the foraging assay (Sarnelle & Wilson 2008). Note that here we do not correct for host size in order to maintain more variation in foraging rates among different size classes of hosts (f instead of $\hat{f}$).

We also calculated foraging rates of the same hosts in terms of parasite consumption (f_Z). In short, we stained media in the tubes with dye, filtered it onto filter paper, mounted the filter papers on slides, and counted parasites with a compound microscope. We used a cotton blue dye that binds to the chitin of fungal cell walls (0.05 g methyl blue dye powder dissolved overnight in 40 mL DI water, mixed with 40 mL of lactic acid). We added 1 mL of dye per 10 mL of sample and let samples stain overnight at 4C. Then, we filtered each sample onto a membrane filter (Pall Supor-200 0.2µm 25mm) placed over an A/E glass fiber filter. The bottom layer of the glass fiber filer helps yield homogenous samples. Finally, we mounted the membrane filters onto microscope slides with emersion oil and counted spores (Z_{count}) with a compound microscope (units: spores per field of vision). We counted spores in both control (ungrazed) and experimental (grazed) tubes and calculated foraging rate exactly as before, but substituted spore counts (Z_{count}) for the fluorescence of algae (A): $f_Z = \ln\left(\frac{ungrazed\ Z_{count}}{grazed\ Z_{count}}\right)\frac{V}{t}$.

We plotted foraging rates that we calculated in terms of algal consumption (f_A) versus foraging rates that we calculated in terms of spore consumption (f_Z; Fig. S1). We assessed the tightness of the relationship as a linear model and asked whether its slope deviated from the 1:1 line using the package car (Fox & Weisberg 2011). Foraging rate measured as algal consumption explained 42% of the variation in foraging rates that were measured as spore consumption. Moreover, the slope of this relationship did not significantly deviate from 1. Therefore, consumption of *Ankistrodesmus* algae by *D. dentifera* hosts serves as an accurate proxy for the consumption *M. bicuspidata* spores. Since measuring the relative fluorescence of algae is much simpler and faster than staining and counting spores, we typically calculate foraging rate in terms of relative algal fluorescence.

Fig. S1. ***Foraging rate measured as the consumption of algae serves as an accurate proxy for the consumption of fungal spores.*** Consumption of *Ankistrodesmus sp.* algae (f_A) correlates strongly with the consumption of *M. bicuspidata* spores (f_Z) by *Daphnia dentifera* hosts (R^2 = 0.42). The slope of this relationship does not significantly deviate from 1 (*p* = 0.21).

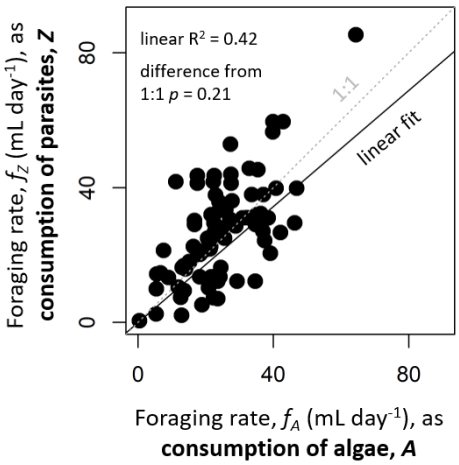

Model fitting details

We fit each transmission model (eqs. 1-4 with each combination of *F* and *U* from Table 2; models A-L) using maximum likelihood. Our likelihood function incorporated three sources of data: fluorescence of experimental tubes from the foraging assay ($A_{observed}$), infection status of hosts from the infection assay ($I_{observed}$), and body size of each host (*L*). A tractable analytical solution only existed for the simplest transmission function: constant *F* and constant *U* (model I). Therefore, we simulated numeric solutions to eqs. 1-4 using the deSolve package in R (Soetaert *et al.* 2010; R Core Team 2017). We set initial conditions to match the experiment: susceptible hosts $S_{initial}$ = 1/15mL; infected hosts $I_{initial}$ = 0; parasite spores $Z_{initial}$ = 0, 75, 200, or 393/mL; algae $A_{initial}$ = mean fluorescence of the ungrazed controls (*in vivo* chlorophyll *a*). We simulated until time *t* (the duration of each genotype's foraging assay) and recorded the final values of infected hosts I_{final} and algae A_{final}.

We set minimum foraging rate (f_{min}) to a constant, because we could not fit this parameter to all genotypes. In the first round of the experiment, we only measured foraging rate at two parasite densities. With only these two points, we could not fit an intercept ($\hat{f}_0$), slope (α), and minimum (f_{min}) to the foraging data. Instead, we set minimum foraging rate (f_{min}) to the 2.5% percentile of empirically observed mean foraging rates across genotypes and parasite densities (3.6 mL day^{-1}). This assumption adequately

fit the two genotypes where minimum foraging rates became relevant: “Bristol 10” (Fig. 1G) and “Island 278” in round two (Fig. S3).

We fit our model parameters (2-4 per genotype, depending on the transmission model) using the Nelder-Mead optimizer in the bbmle package in R (Bolker 2008; R Core Team 2017). We assumed that residuals of the log-transformed fluorescence data ($A_{observed}$-A_{final}) were normally distributed (Sarnelle & Wilson 2008) with standard deviations fitted to the foraging residuals of each genotype-round combination. Therefore, in addition to estimating the two biological foraging parameters ($\hat{f}_0$ and α), we also estimated statistical foraging parameters (standard deviations of foraging residuals), which also counted against AIC scores of each model (see “#Parameters” in Table 1). We assumed that the infection data ($I_{observed}$) were binomially distributed. We summed the log-likelihoods across all genotypes to calculate overall AIC scores for each model.

Empirical data and transmission functions fit to all host genotypes

Figures S2, S3, & S4. *Empirical data and transmission functions fit to all host genotypes.* Points (with standard errors) show empirical data from the joint foraging/infection assay. Lines plot transmission functions (Table 2) over the density gradient of parasite spores, *Z*. Exposure, *F*, is fit to the foraging assay (top row), the transmission coefficient (β) is fit to the infection assay (middle row), and per-parasite susceptibility, *U*, is fit as β / F (bottom row). Columns show each host genotype, ordered by round of the experiment (R1, R2 and R3). The best overall model includes exponential exposure and exponential susceptibility (thick solid blue; Table 2, model A). Also plotted: constant exposure & constant susceptibility (thin solid gold; model I), exponential exposure & constant susceptibility (dotted green; model C), constant exposure & exponential susceptibility (dashed purple; model G). Other combinations are not displayed. Three illustrative genotypes also in Fig. 1; parameters listed in Tables S2-S3.

Figure S2.

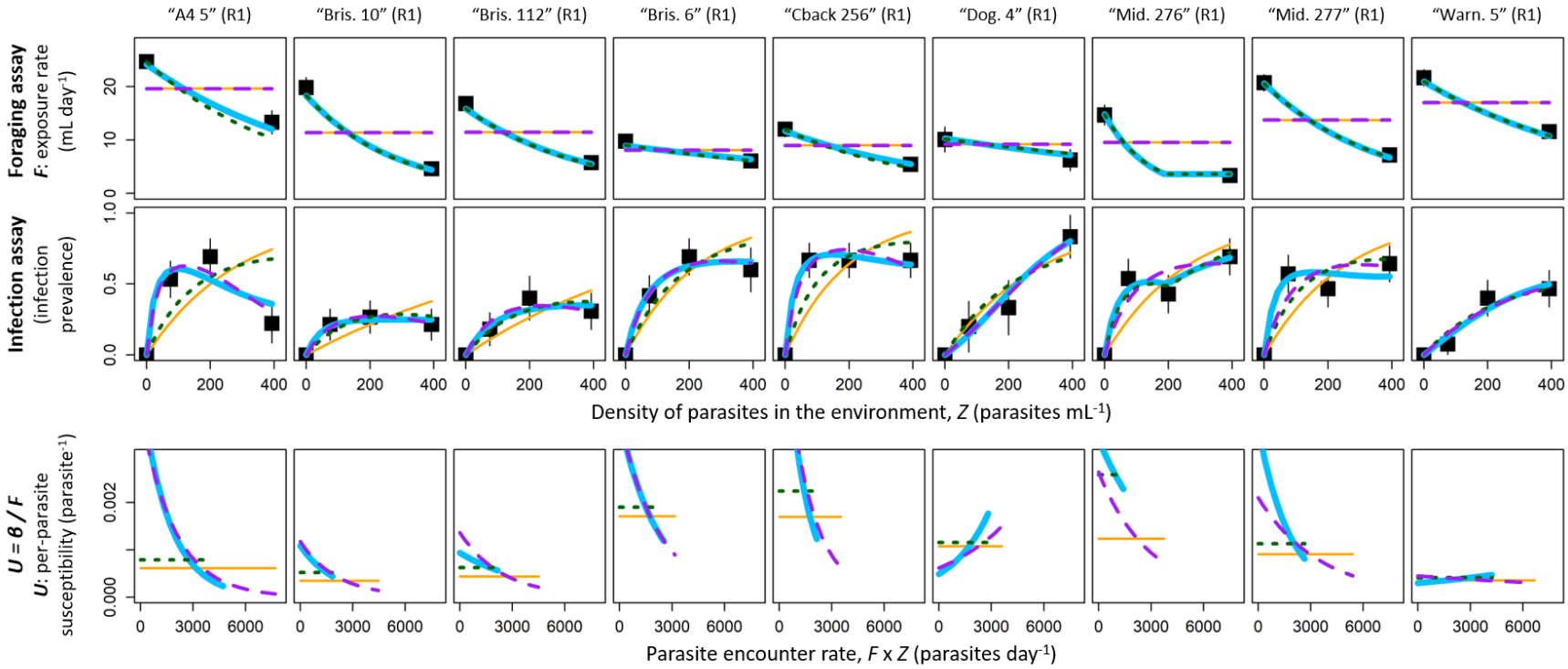
"A4 5" (R1)
"Bris. 10" (R1)
"Bris. 112" (R1)
"Bris. 6" (R1)
"Cback 256" (R1)
"Dog. 4" (R1)
"Mid. 276" (R1)
"Mid. 277" (R1)
"Warn. 5" (R1)
Foraging assay
F: exposure rate (mL day-1)
Infection assay (infection prevalence)
Density of parasites in the environment, Z (parasites mL-1)
U = β / F
U: per-parasite susceptibility (parasite-1)
Parasite encounter rate, F x Z (parasites day-1)

Figure S3.

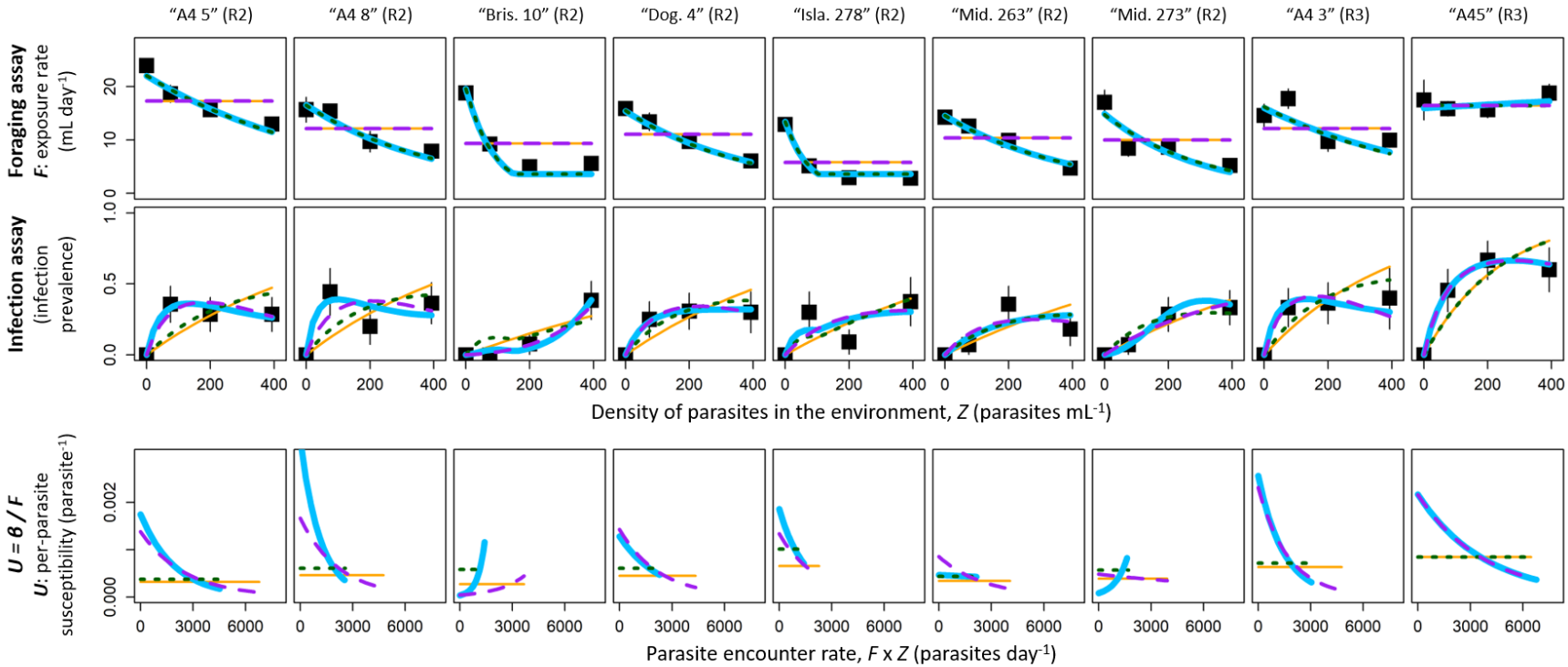
"A4 5" (R2)
"A4 8" (R2)
"Bris. 10" (R2)
"Dog. 4" (R2)
"Isla. 278" (R2)
"Mid. 263" (R2)
"Mid. 273" (R2)
"A4 3" (R3)
"A45" (R3)
Foraging assay
F: exposure rate (mL day-1)
Infection assay (infection prevalence)
Density of parasites in the environment, Z (parasites mL-1)
U = β / F
U: per-parasite susceptibility (parasite-1)
Parasite encounter rate, F x Z (parasites day-1)

Figure S4.

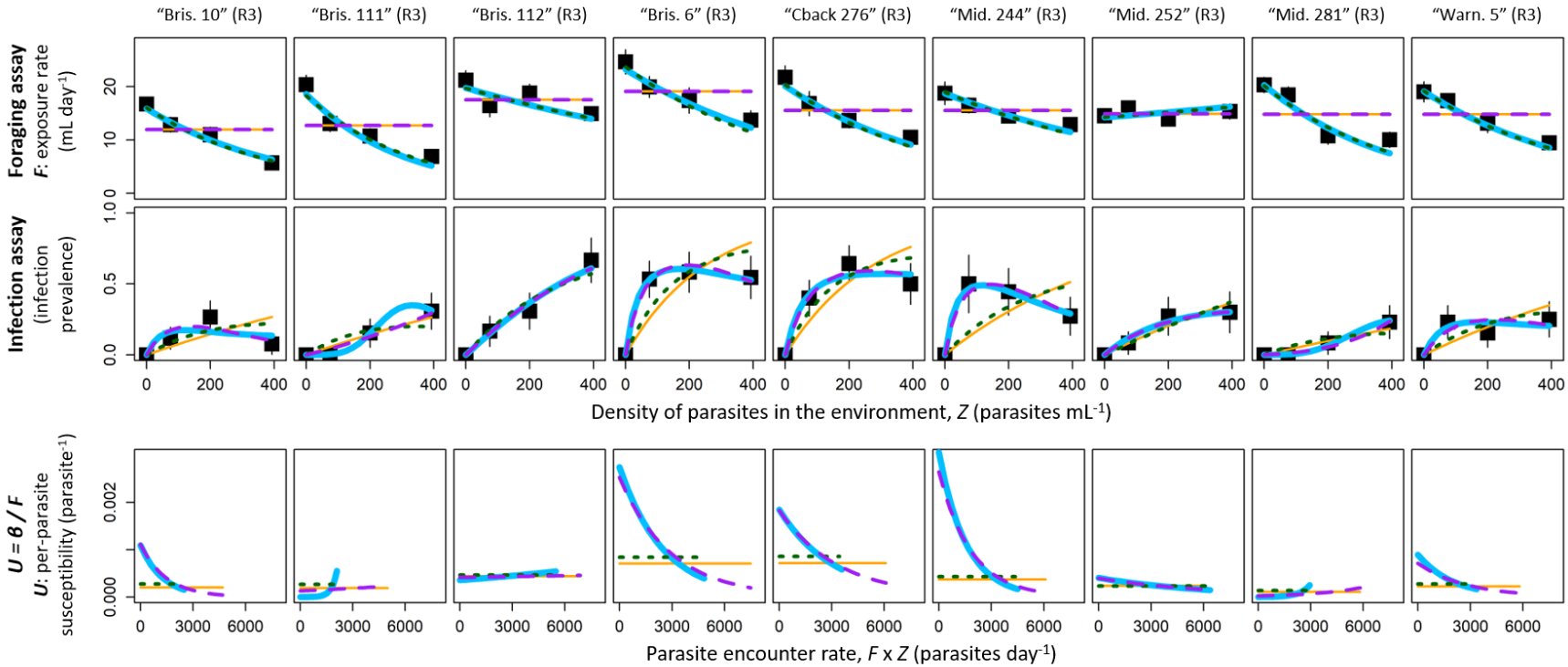
"Bris. 10" (R3)
"Bris. 111" (R3)
"Bris. 112" (R3)
"Bris. 6" (R3)
"Cback 276" (R3)
"Mid. 244" (R3)
"Mid. 252" (R3)
"Mid. 281" (R3)
"Warn. 5" (R3)
Foraging assay
F: exposure rate (mL day-1)
Infection assay (infection prevalence)
Density of parasites in the environment, Z (parasites mL-1)
U = β / F
U: per-parasite susceptibility (parasite-1)
Parasite encounter rate, F x Z (parasites day-1)

Parameters and confidence intervals

Table S2. *Exposure (F) parameters, accompanied by 95% confidence intervals (lower and upper) for all genotypes fit by the winning model (exponential F, exponential U [Table 1B; model A]; plotted in Figs. S2-S4; for 'rounds' [R] 1-3). Parameters:* $\hat{f}_0$ *is background size-specific exposure/foraging rate with zero parasites; α is the coefficient of exposure plasticity (Table 1). L is mean body size (length) of hosts.*

R	genotype	$\hat{f}_0$ (mL day^{-1} mm^{-2})			α (mL parasite^{-1} mm^{-2})			L
		estimate	lower	upper	estimate	lower	upper	(mm)
1	A4 5	16.43	14.65	18.35	-1.21E-3	-1.88E-3	-6.31E-4	1.21
1	Bristol 10	14.11	11.88	16.43	-2.80E-3	-8.46E-3	-2.09E-3	1.14
1	Bristol 112	12.98	11.35	14.67	-2.21E-3	-3.26E-3	-1.64E-3	1.10
1	Bristol 6	5.89	4.65	7.08	-5.55E-4	-1.44E-3	1.47E-4	1.23
1	Canvasback 256	11.71	9.53	13.83	-1.94E-3	-7.33E-3	-1.10E-3	1.00
1	Dogwood 4	7.34	4.54	9.64	-6.56E-4	-9.60E-3	3.14E-4	1.18
1	Midland 276	15.09	12.18	17.36	-7.68E-3	-1.03E-2	-2.19E-3	0.99
1	Midland 277	18.43	16.23	20.41	-2.57E-3	-3.59E-3	-1.84E-3	1.06
1	Warner 5	14.85	12.99	16.77	-1.21E-3	-1.58E-3	-8.57E-4	1.19
2	A4 5	14.60	13.27	15.96	-1.09E-3	-1.55E-3	-6.75E-4	1.23
2	A4 8	13.38	11.02	16.05	-1.93E-3	-3.53E-3	-1.01E-3	1.11
2	Bristol 10	13.38	11.66	14.85	-7.74E-3	-9.57E-3	-4.16E-3	1.21
2	Dogwood 4	11.37	9.92	13.23	-1.82E-3	-2.58E-3	-1.30E-3	1.16
2	Island 278	11.89	10.08	13.64	-1.17E-2	-4.48E-2	-7.57E-3	1.06
2	Midland 263	12.37	11.43	13.42	-2.12E-3	-2.98E-3	-1.59E-3	1.08
2	Midland 273	11.71	9.47	15.71	-2.65E-3	-1.13E-2	-1.58E-3	1.13
3	A4 3	7.68	6.30	9.35	-8.87E-4	-1.42E-3	-4.33E-4	1.44
3	A4 5	6.95	5.37	8.74	8.55E-5	-4.02E-4	5.75E-4	1.52
3	Bristol 10	8.47	7.57	9.37	-1.24E-3	-1.66E-3	-9.13E-4	1.37
3	Bristol 111	8.72	7.54	9.89	-1.53E-3	-2.65E-3	-1.00E-3	1.46
3	Bristol 112	9.10	7.77	10.49	-4.06E-4	-6.77E-4	-1.21E-4	1.47
3	Bristol 6	11.83	10.24	13.51	-8.24E-4	-1.30E-3	-4.07E-4	1.40
3	Canvasback 276	10.98	9.34	12.74	-1.10E-3	-1.59E-3	-6.54E-4	1.35
3	Midland 244	9.38	7.87	10.98	-6.25E-4	-1.01E-3	-2.46E-4	1.41
3	Midland 252	7.64	6.71	8.61	1.80E-4	-2.02E-4	5.48E-4	1.36
3	Midland 281	9.69	8.53	10.77	-1.21E-3	-1.62E-3	-7.63E-4	1.45
3	Warner 5	10.14	8.76	11.59	-1.09E-3	-1.55E-3	-6.90E-4	1.37

Table S3. *Per-parasite susceptibility (U) parameters, accompanied by 95% confidence intervals (lower and upper) for all genotypes fit by the winning model (exponential F, exponential U [Table 1B; model A]; plotted in Figs. S2-S4; for 'rounds' [R] 1-3). Parameters:* μ_0 *is background per parasite susceptibility with zero parasites; w is the coefficient of susceptibility plasticity (Table 1).*

R	genotype	u_0 (parasite^{-1})			w (mL parasite^{-1})		
		estimate	lower	upper	estimate	lower	upper
1	A4 5	4.39E-3	1.58E-3	1.24E-2	-6.20E-4	-1.01E-3	-2.78E-4
1	Bristol 10	1.09E-3	6.29E-7	1.34E-2	-4.90E-4	-2.57E-3	3.79E-3
1	Bristol 112	9.36E-4	2.16E-7	5.58E-3	-2.35E-4	-1.30E-3	5.34E-3
1	Bristol 6	3.76E-3	9.77E-4	1.13E-2	-4.57E-4	-1.16E-3	4.95E-4
1	Canvasback 256	7.43E-3	2.44E-3	2.48E-2	-8.37E-4	-1.84E-3	-7.12E-5
1	Dogwood 4	4.89E-4	1.25E-9	3.59E-3	4.56E-4	-5.10E-4	9.33E-3
1	Midland 276	3.33E-3	5.66E-4	2.07E-2	-2.66E-4	-2.07E-3	1.23E-3
1	Midland 277	3.58E-3	7.07E-4	2.21E-2	-5.61E-4	-1.68E-3	1.63E-4
1	Warner 5	3.00E-4	2.62E-5	1.13E-3	1.07E-4	-3.28E-4	8.49E-4
2	A4 5	1.75E-3	2.99E-4	7.92E-3	-5.11E-4	-1.22E-3	4.08E-6
2	A4 8	3.34E-3	1.25E-4	1.14E-1	-8.80E-4	-3.67E-3	6.98E-4
2	Bristol 10	3.55E-5	1.17E-12	5.74E-4	2.47E-3	-1.36E-4	1.51E-2
2	Dogwood 4	1.28E-3	1.91E-5	6.69E-3	-4.39E-4	-1.54E-3	2.19E-3
2	Island 278	1.86E-3	6.88E-5	1.99E-2	-6.83E-4	-5.03E-3	2.21E-3
2	Midland 263	4.66E-4	7.70E-6	2.55E-3	-4.01E-5	-1.19E-3	2.55E-3
2	Midland 273	8.03E-5	3.43E-8	1.96E-3	1.43E-3	-9.65E-4	7.06E-3
3	A4 3	2.56E-3	2.76E-4	1.40E-2	-6.94E-4	-1.96E-3	3.45E-4
3	A4 5	2.17E-3	7.27E-4	5.80E-3	-2.63E-4	-5.61E-4	3.17E-5
3	Bristol 10	1.09E-3	8.28E-5	5.12E-3	-7.84E-4	-1.98E-3	4.37E-4
3	Bristol 111	4.22E-7	9.84E-13	1.59E-4	3.43E-3	8.63E-6	1.05E-2
3	Bristol 112	3.58E-4	3.65E-5	1.25E-3	7.59E-5	-2.88E-4	6.50E-4
3	Bristol 6	2.74E-3	8.51E-4	7.82E-3	-4.02E-4	-8.01E-4	-3.46E-5
3	Canvasback 276	1.84E-3	4.82E-4	5.78E-3	-3.21E-4	-8.44E-4	1.80E-4
3	Midland 244	3.06E-3	4.69E-4	1.66E-2	-6.44E-4	-1.39E-3	-1.01E-4
3	Midland 252	4.05E-4	3.40E-5	1.50E-3	-1.58E-4	-6.36E-4	4.25E-4
3	Midland 281	1.58E-6	2.13E-13	1.10E-4	1.72E-3	-2.20E-4	7.45E-3
3	Warner 5	8.94E-4	2.93E-5	6.58E-3	-5.03E-4	-1.68E-3	7.35E-4

Additional correlations

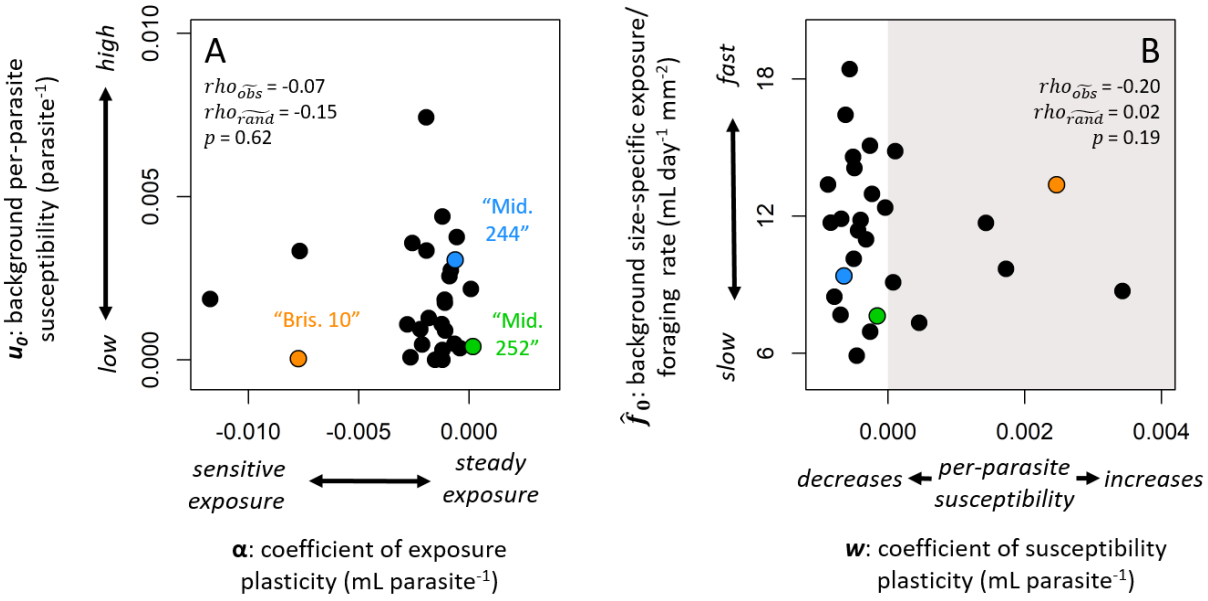

Figure S5. *Additional correlations between parameters from the winning model (model A).* Points are genotypes including the illustrative examples in Fig 1 from the main text. *P* values indicate the proportion of randomized Spearman correlations (with median $rho_{\widetilde{rand}}$) that are more extreme than the observed correlation ($rho_{\widetilde{obs}}$). The other pairwise correlations are depicted in Fig. 3 in the main text. **A)** Background per-parasite susceptibility (u_0) does not correlate with the coefficient of exposure plasticity (α). **B)** The coefficient of susceptibility plasticity (w) does not correlate with background exposure/ foraging rate in the absence of parasites ($\hat{f}_0$). Note: Parameters are plotted for all genotypes in all rounds, but the correlation statistics account for pseudoreplication by including only a single parameter set per genotype. The observed correlation $rho_{\widetilde{obs}}$ is the median among all combinations of the 19 genotypes.

Graphical depiction of round-to-round variation

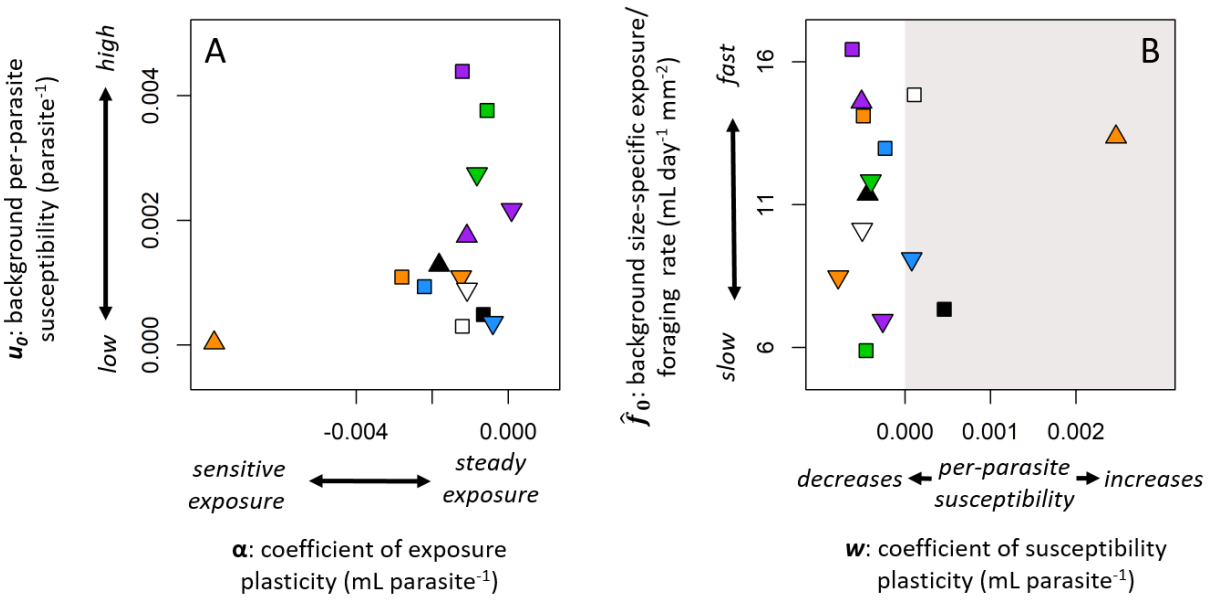

Figure S6. *Graphical depiction of round-to-round variation.* Points are parameters of genotypes that were repeated among rounds of the experiment, including "A45" (purple), "Bristol 10" (orange), "Bristol 6" (green), "Bristol 112" (blue), "Warner 5" (white), and "Dogwood 4" (black). Genotypes that were not repeated are not depicted here. Symbols indicate rounds of the experiment: round 1 (squares), round 2 (upwards triangles) or round 3 (downwards triangles). The two pairwise correlation plots (analogous to Fig. S5, but highlighting the round-to-round variation) enable a visual representation of round-to-round variation for parameters including the coefficient of exposure plasticity (α; x-axis, panel A), background per-parasite susceptibility (u_0; y-axis, panel A), the coefficient of susceptibility plasticity (w; x-axis, panel B), and background exposure/ foraging rate in the absence of parasites ($\hat{f}_0$; y-axis, panel B).

Correlations among parameters from the winning model

We detected two correlations among pairs of parameters from the winning model. For this analysis, we used the best model (model A), which fit a unique set of parameters to each genotype in each round of the experiment. However, using all of these parameters together would bias the correlation statistics, since some genotypes were repeated among rounds of the experiment. Therefore, to avoid pseudoreplication, we selected one set of parameters per genotype, and calculated the observed correlations for all possible combinations of the 19 genotypes. Since two genotypes were repeated among three rounds and four genotypes were repeated among two rounds, this procedure created 3 x 3 x 2 x 2 x2 = 144 combinations of all 19 genotypes. We report the median of these 144 observed Spearman correlations for each relationship ($rho_{\widetilde{obs}}$). We also report the median Spearman correlations to arise from randomized data for each relationship ($rho_{\widetilde{rand}}$). The randomized correlations are important, because they reveal cases where parameters (especially intercepts [e.g., u_0] and slopes [e.g., w]) are expected to covary by chance (Schielzeth 2010). Finally, we report as *p* values the proportion of randomizations that produced more extreme correlations than the median correlation that we observed.

Two pairs of parameters correlated strongly, but only one relationship was significantly stronger than expected by chance. The two susceptibility parameters (w and u_0) correlated strongly and negatively, but this relationship was consistent with the randomized data. Therefore, this correlation likely reflects a statistical property of models that fit slopes and intercepts for per-parasite susceptibility *U*. The strength of this correlation could also reflect the relatively low statistical power of the infection data (~50 Bernoulli trials per genotype per round). On the other hand, the two exposure parameters ($\hat{f}_0$ and α) correlated more strongly and negatively than 95% of the randomizations ($p < 0.05$). Therefore, this relationship likely reflects a biological (rather than statistical) pattern, and could indicate a tradeoff between biological traits. Specifically, foraging/exposure (*F*) ranged from 'fast and sensitive' (large $\hat{f}_0$,

negative α) to 'slow and steady' (small $\hat{f}_0$, α near 0). This relationship was robust whether using the median or mean of the observed correlations ($rho_{\widetilde{obs}}$), because the distribution of observed correlations between $\hat{f}_0$ and α was normally distributed (Shapiro Wilk p = 0.12) with nearly identical median (*rho* = -0.701) and mean (*rho* = -0.708).

Table S3. *Correlations among parameters from the winning model* (exponential *F*, exponential *U*; Table 1A; Fig. 3 and S5). *Parameters: $\hat{f}_0$ is background size-specific exposure (i.e., foraging) rate with zero parasites; α is the coefficient of exposure plasticity; μ_0 is background per parasite susceptibility (with zero parasites); w is the coefficient of susceptibility plasticity (Table 1).*

relationship	**fig.**	$rho_{\widetilde{obs}}$	$rho_{\widetilde{rand}}$	*p value**
$\hat{f}_0 - \alpha$	3A	-0.701	-0.395	**0.038**
$w - \alpha$	3B	0.029	0.211	0.76
$\hat{f}_0 - u_0$	3C	0.316	-0.011	0.084
$w - u_0$	3D	-0.835	-0.881	0.74
$\alpha - u_0$	S5A	-0.070	-0.147	0.62
$w - \hat{f}_0$	S5B	-0.197	0.021	0.185

*We asked how frequently the randomized data (with median $rho_{\widetilde{rand}}$) produced correlations that were more extreme than the median observed correlations ($rho_{\widetilde{obs}}$). The direction of this test depended on the sign of the observed correlation.

Early host death

The statistical analysis presented in the main text excludes hosts that died before we could diagnose infections (five or fewer days after exposure). Omitting these hosts removed 136 of 1,492 observations from the infection data (< 10%). The mean number of replicates for each genotype-round combination (across parasite density treatments) dropped from 55.2 to 50.2. Extensive mortality prior to diagnosis can bias estimates of transmission rates (KE Shaw and DJ Civitello, unpublished data) because it can confound parasite transmission and virulence. In this analysis, increasing early mortality at higher

parasite densities could theoretically negatively bias our estimate of the coefficient of susceptibility plasticity, *w*. Specifically, if a large proportion of hosts died at the highest parasite densities before we could diagnose their infections, then infection prevalence of the remaining hosts could appear artificially low. This pattern – if it existed – could lead to negative estimates of *w* (therefore, *U* would decline with *Z* more than it should). To evaluate this possibility, we fit a complementary model using our winning functions for *F* and *U* that also accounted for early host deaths.

The complementary model replaces the binomial-based likelihood function for the infection data with a multinomial-based function. Both approaches begin by calculating infection prevalence of the hosts (as in the main text), according to the functions for exposure (*F*) and per-parasite susceptibility (*U*). Then, for the time period between exposure and the earliest possible detection of infections, the multinomial-based function classifies each host as 1) alive and infected, 2) alive and uninfected, or 3) already dead. Probabilities for these three categories are calculated, respectively, as

1. $prevalence * exp\big(-t\ (d + v)\big)$ eq. S1
2. $(1 - prevalence) * exp(-t\ \ d)$ eq. S2
3. $prevalence * \Big(1 - exp\big(-t\ (d + v)\big)\Big) + (1 - prevalence) * \big(1 - exp(-t\ d)\big)$ eq. S3

where *d* represents the daily background mortality rate, and *v* represents the additional mortality rate caused by parasite virulence for infected hosts. This representation of morality is used extensively in epidemiological models. Both rates *d* and *v* are expressed in units day^{-1}, where *t* represents the time between exposure and the earliest possible diagnosis of infection. Therefore, equation S1 is the proportion infected (*prevalence*) times survival to time *t*, given enhanced mortality $(d + v)$, where survival is $exp\big(-t\ (d + v)\big)$. In equation S2, observation of uninfected hosts at time *t* is the probability of being uninfected (1-*prevalence*) times the probability of surviving to time *t*, given lower background mortality, *d*. Equation S3, then, is the sum of probabilities of dying (i.e., not surviving) as an infected hosts

$1 - exp\big(-t\ (d + v)\big)$ or an uninfected host $1 - exp(-t\ d)$. Thus, this approach accounts for early death by fitting *d* and *v* in the same likelihood function as *F* and *U*. If there is substantial early host mortality, but it is unrelated to parasite density, then this approach would estimate a large (i.e., statistically nonzero) value for *d*. If host mortality increases with parasite density, then this approach would estimate a large (i.e., statistically nonzero) value for *v*. In either case, simulation studies indicate that the occurrence of early mortality does not negatively bias estimates of *u* or *w* (KE Shaw and DJ Civitello, unpublished data).

Several genotype-round combinations exhibited no early mortality. In these cases this approach is unnecessary - it would mere estimate *d* = *v* = 0 and recover our original parameter estimates. We fit this combined transmission-mortality model to the remaining genotype-round combinations that did exhibit early mortality. The fitted functions for exposure and per-parasite susceptibility were almost identical to the functions fit by models that omitted early deaths. Twenty hosts showed decreasing per-parasite susceptibility over the gradient of parasite density (negative *w*'s) in the primary model, and nineteen of these hosts still showed decreasing per-parasite susceptibility in the early death model. The w's correlated very strongly between these two models (linear R^2 = 0.861). Thus, omitting hosts that died before we could diagnose infections did not bias our results.

REFERENCES FOR APPENDIX

1.

Bates, D., Mächler, M., Bolker, B. & Walker, S. (2015). Fitting Linear Mixed-Effects Models Using lme4. *2015*, 67, 48.

2.

Bolker, B.M. (2008). *Ecological Models and Data in R*. Princeton University Press.

3.

Fox, J. & Weisberg, S. (2011). *An R Companion to Applied Regression*. SAGE Publications.

4.

R Core Team (2017). R: A language and environment for statistical computing. R Foundation for Statistical Computing Vienna, Austria.

5.

Sarnelle, O. & Wilson, A.E. (2008). Type III functional response in Daphnia. *Ecology*, 89, 1723-1732.
6.

Schielzeth, H. (2010). Simple means to improve the interpretability of regression coefficients. *Methods Ecol. Evol.*, 1, 103-113.
7.

Soetaert, K., Petzoldt, T. & Setzer, R.W. (2010). Solving differential equations in R: Package deSolve. *J. Stat. Softw.*, 33, 1-25.